# Molecular Transport Junctions: Asymmetry in Inelastic Tunneling Processes †

**ARTICLE** *in* THE JOURNAL OF PHYSICAL CHEMISTRY B · JUNE 2005

Impact Factor: 3.3 · DOI: 10.1021/jp0457500 · Source: PubMed



**4 AUTHORS**, INCLUDING:

Michael Galperin
University of California, San Diego
**82** PUBLICATIONS **2,472** CITATIONS
SEE PROFILE

Mark A. Ratner
Northwestern University
**905** PUBLICATIONS **41,521** CITATIONS
SEE PROFILE

Duncan Stewart
National Research Council Canada
**70** PUBLICATIONS **7,162** CITATIONS
SEE PROFILE

# Molecular Transport Junctions: Asymmetry in Inelastic Tunneling Processes†

**Michael Galperin,*,‡ Abraham Nitzan,§ Mark A. Ratner,‡ and Duncan R. Stewart‖**

*Department of Chemistry and Materials Research Center, Northwestern University, Evanston, Illinois 60208, School of Chemistry, The Sackler Faculty of Science, Tel Aviv University, Tel Aviv 69978, Israel, and Hewlett-Packard Laboratories, Palo Alto, CA*

*Received: September 18, 2004; In Final Form: January 21, 2005*

Inelastic electron tunneling spectroscopy (IETS) measurements are usually carried out in the low-voltage ("Ohmic", i.e., linear) regime where the elastic conduction/voltage characteristic is symmetric to voltage inversion. Inelastic features, normally observed in the second derivative $d^2I/dV^2$ are also symmetric (in fact antisymmetric) in many cases, but asymmetry is sometimes observed. We show that such asymmetry can occur because of different energy dependences of the two contact self-energies. This may be attributed to differences in contact density of states (different contact material) or different energy dependence of the coupling (STM-like geometry or asymmetric positioning of molecular vibrational modes in the junction). The asymmetry scales with the difference between the energy dependence of these self-energies and disappears when this dependence is the same for the two contacts. Our nonequilibrium Green function approach goes beyond proposed WKB scattering theory[1] in properly accounting for Pauli exclusion, as well as providing a path to generalizations, including consideration of phonon dynamics and higher-order perturbation theory.

Rectification effects in molecular conduction junctions have been of interest both for possible diode device applications of such junctions[2] (where voltage dependence of the donor and acceptor (contacts) energy levels brings them in or out of resonance at opposite voltage drop polarities) and because of the need to understand the bias asymmetry in scanning tunneling microscope studies of adsorbed molecules[3]. Current−voltage ($I/V$) asymmetry can arise from different electronic structure in the contacts (peaks in density of states) or from an asymmetric behavior with respect to bias inversion of the electrostatic potential distribution across the junction. The latter can be caused by geometric asymmetry, different coupling strength of the molecule to the contacts, weak links, and charging.[4,5] In such cases, change of the electronic structure of the molecule under bias reversal is responsible for the rectification.

In inelastic electron tunneling spectroscopy (IETS), one follows the onset of inelastic effects on the tunneling current that are most pronounced in the second derivative of current vs voltage.[6] Here we consider the possible asymmetry of $d^2I/dV^2$ under a similar voltage reversal. Note that mechanisms for $I-V$ asymmetry mentioned above work in the relatively high-voltage regime (of the order of LUMO−HOMO gap), after essential current buildup starts. IETS experiments, on the other hand, are done at much lower voltages in the "Ohmic" (by "Ohmic", we designate current−voltage characteristics) regime. Naively speaking, "Ohmic" behavior would suggest a symmetric signal in this case. On the other hand, the inelastic character of the measurement suggests that strict invariance to bias reversal holds only for the symmetric positioning of the vibrational mode between the electrodes. Indeed, the simplest picture for the IETS experiment is just an electron tunneling through a rectangular barrier and interacting with a phonon (vibration) at some point. An electron that loses energy (the only possibility at low temperature) to the vibrational mode will tunnel the rest of its way at lower energy, thus with lower tunneling probability. Therefore, the overall tunneling probability for an electron going from left to right as compared to the opposite direction should depend on the position of the vibrational mode in the rectangular barrier. For example, if the molecule is situated closer to the left electrode, the left-to-right inelastic tunneling probability at a given energy is expected to be smaller than the right-to-left transmission probability at the same energy. It should be emphasized that the mechanism for asymmetry is specific to the inelastic part of the $I/V$ signal. This mechanism will remain, and asymmetry can occur in IETS, even when the elastic $I/V$ behavior is symmetric.

A theory of vibrational mode intensities in IETS signals was earlier proposed at the level of a WKB scattering approach by Kirtley and co-workers[1]. The influence of the Fermi statistics in the leads (Pauli principle) on the inelastic process was disregarded in that work; here, we consider it. Our approach (though not implemented here) can go beyond the second order of perturbation theory (golden rule) and also makes it possible to extend the treatment to take into account the influence of the electronic subsystem on the phonon dynamics and vice versa (for detailed discussion see Ref 8).

In the language of quantum mechanics of open systems, the physics of asymmetry in electron transmission probability expresses itself through the energy dependence of the corresponding self-energies. As an example, let us consider a single molecular site represented by a single level coupled to the left and right ($L$ and $R$) contacts and to the local phonon. The Hamiltonian ($\hbar \equiv 1$) is then

$$\hat{H} = E_0\hat{c}^\dagger\hat{c} + \sum_{k\in\{L,R\}} \epsilon_k \hat{d}_k^\dagger \hat{d}_k + \omega_0 \hat{a}^\dagger\hat{a} + \sum_{k\in\{L,R\}} \left(V_k \hat{c}^\dagger \hat{d}_k + \overset{*}{V}_k \hat{d}_k^\dagger \hat{c}\right) + M(\hat{a}^\dagger + \hat{a})\hat{c}^\dagger\hat{c} \quad (1)$$

Here $E_0$, $\epsilon_k$, $\omega_0$, $V_k$ and $M$ are, respectively, the electronic site energy, the electronic energy levels in the metal (i.e., leads),

† Part of the special issue "George W. Flynn Festschrift".

* Author to whom correspondence should be addressed. E-mail: misha@chem.northwestern.edu.

‡ Northwestern University.

§ Tel Aviv University.

‖ Hewlett-Packard Laboratories.

10.1021/jp0457500 CCC: $30.25 
Published on Web 00/00/0000 PAGE EST: 3.5

the phonon frequency, the coupling between electrode and molecular electronic levels, and the vibronic coupling energy. The operators $\hat{c}^\dagger$ and $\hat{d}_k^\dagger$ create electrons in the molecular level and in the electrode k-states, while $\hat{a}^\dagger$ creates a phonon.

In the lowest order, the lesser and greater self-energies due to coupling to the phonon are[8]

$$\Sigma_{ph}^{<,>}(E) = iM^2 \int \frac{d\omega}{2\pi} D_0^{<,>}(\omega) G_0^{<,>}(E-\omega) \tag{2}$$

Here $D_0^{<,>}$ and $G_0^{<,>}$ are zero-order (in electron−phonon interaction) Green functions

$$D_0^{<}(\omega) = D_0^{>}(-\omega) = \begin{cases} -i[1+N(|\omega|)]\rho_{ph}(|\omega|) & \omega < 0 \\ -iN(\omega)\rho_{ph}(\omega) & \omega > 0 \end{cases}$$

$$G_0^{<}(E) = \{if_L(E)\Gamma_L(E) + if_R(E)\Gamma_R(E)\}|G_0^{\mathrm{r}}(E)|^2$$

$$G_0^{>}(E) = \{-i[1-f_L(E)]\Gamma_L(E) - i[1-f_R(E)]\Gamma_R(E)\}|G_0^{\mathrm{r}}(E)|^2 \tag{3}$$

where ($K = L, R$)

$$|G_0^{\mathrm{r}}(E)|^2 = [(E-E_0)^2 + (\Gamma(E)/2)^2]^{-1}$$

$$\Gamma_K(E) = 2\pi \sum_{k\in K} |V_k|^2 \delta(E-\epsilon_k)$$

$$f_K(E) = \left[\exp\left(\frac{E-\mu_K}{k_{\mathrm{B}}T}\right) + 1\right]^{-1}$$

$$N(\omega) = \left[\exp\left(\frac{\omega}{k_{\mathrm{B}}T}\right) - 1\right]^{-1}$$

$$\rho_{ph}(\omega) = \gamma_{ph}/[(\omega-\omega_0)^2 + (\gamma_{ph}/2)^2] \tag{4}$$

and where for simplicity, we have neglected the real part of the retarded self-energy due to coupling to the contacts as well as the retarded self-energy due to electron−phonon coupling. Using eq 3 in eq 2 yields (in the noncrossing approximation[7]) the phononic addition to the lesser and greater Green functions

$$G_{ph}^{<,>}(E) = G_0^{\mathrm{r}}(E)\Sigma_{ph}^{<,>}(E)G_0^{\mathrm{a}}(E) \tag{5}$$

which in turn provides the inelastic current[8]

$$I_{\mathrm{inel}} = \frac{2e}{\hbar}\int_{-\infty}^{+\infty}\frac{\mathrm{d}E}{2\pi}[\Sigma_L^{<}(E)G_{ph}^{>}(E) - \Sigma_L^{>}(E)G_{ph}^{<}(E)] \tag{6}$$

$$= \frac{2e}{\hbar}M^2\int_{-\infty}^{+\infty}\frac{\mathrm{d}E}{2\pi}\int_0^{+\infty}\frac{\mathrm{d}\omega}{2\pi}\rho_{ph}(\omega)|G_0^{\mathrm{r}}(E)|^2|G_0^{\mathrm{r}}(E-\omega)|^2$$
$$\{f_L(E)[1-f_R(E-\omega)]\Gamma_L(E)\Gamma_R(E-\omega)$$
$$-f_R(E)[1-f_L(E-\omega)]\Gamma_L(E-\omega)\Gamma_R(E)\} \tag{7}$$

The first term in the curly brackets in eq 7 is responsible for the current at $V = \mu_L - \mu_R > 0$, while the second term contributes at $V < 0$. This contribution to the current is due to inelastic scattering, and it goes to zero when there are no inelastic effects in the junction.[9]

It is evident from eq 7 that asymmetry in the inelastic current (as well as in its second derivative) may be caused by the difference in the energy dependence of $\Gamma_L$ and $\Gamma_R$ in the range between the chemical potentials. Note that the elastic part of the current, whose integrand is proportional to $\Gamma_L(E)\Gamma_R(E)$, is symmetric in this case. Since the inelastic signal in IETS experiments is usually much smaller than the elastic contribution, the asymmetry of eq 7 is most readily observed in the second derivative of current vs voltage rather than in the $I-V$ characteristic. Equation 7 yields

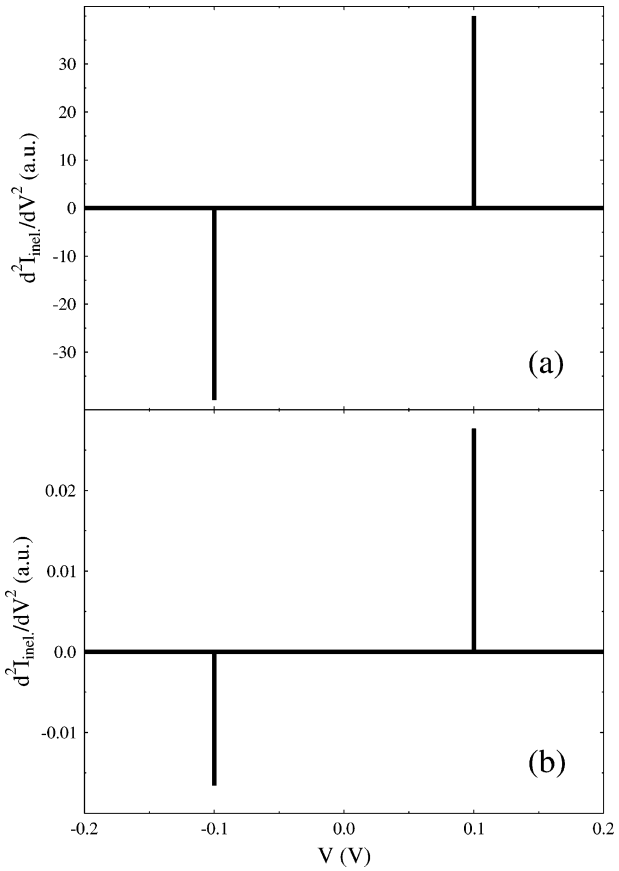


**Figure 1.** $\mathrm{d}^2I/\mathrm{d}V^2$ vs $V$ calculated for the zero-temperature lowest-order result from eq 7. Same energy dependence for both self-energies, gap widths $L_L = L_R = 1$ Å (a), and STM-like setup $L_L = 11$ Å, $L_R = 1$ Å (b).

$$\frac{\mathrm{d}^2I}{\mathrm{d}V^2}(V) \sim \mathrm{sgn}(V)M^2\frac{2e}{\hbar}\rho_{ph}(V)|G_0^{\mathrm{r}}(\mu_L)|^2|G_0^{\mathrm{r}}(\mu_R)|^2\Gamma_L(\mu_L)\Gamma_R(\mu_R) \tag{8}$$

in addition to smooth background terms. Here,

$$\mu_L = E_F + \eta V \qquad \mu_R = E_F - (1-\eta)V \tag{9}$$

where $\eta$ is the voltage division factor.[10] Below, we set $\eta = 0.5$ so as not to confuse the asymmetry effect under consideration with the one caused by an asymmetric electrostatic potential profile across the junction. Since $\rho_{ph}(\omega)$ is highly localized near $\omega_0$, it will determine the voltage dependence of $\mathrm{d}^2I/\mathrm{d}V^2$ according to eq 8. The second derivative will have two peaks at $V = \pm\omega_0$, with widths defined by $\gamma_{\mathrm{ph}}$. Their heights will be determined by $\Gamma_L(E_F \pm \omega_0/2)\Gamma_R(E_F \mp \omega_0/2)$ at $V = \pm\omega_0$ so that different energy dependences of the self-energies indeed lead to asymmetry of the IETS signal under voltage reversal.

In the spirit of the simple picture of electron tunneling through a rectangular double-barrier potential, we assume an energy dependence of the retarded self-energy due to coupling (its imaginary part) to contacts in the form

$$\Gamma_K(E) = A_K \exp\left(-2\sqrt{\frac{2m}{\hbar^2}(U_K - E)}L_K\right) \qquad K = L, R \tag{10}$$

Disregarding the possible difference between $U_L$ and $U_R$, a

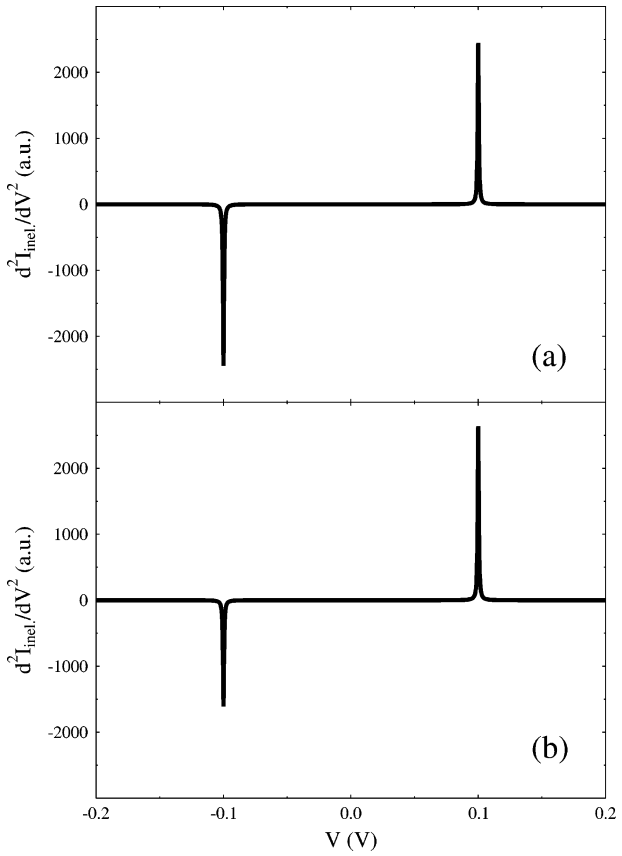


**Figure 2.** $d^2I/dV^2$ vs $V$ calculated for the zero-temperature lowest-order result from eq 8, Newns−Anderson model. $E_L = E_R = 0$ eV (a), $E_L = 0.4$ eV, and $E_R = 0$ eV (b).

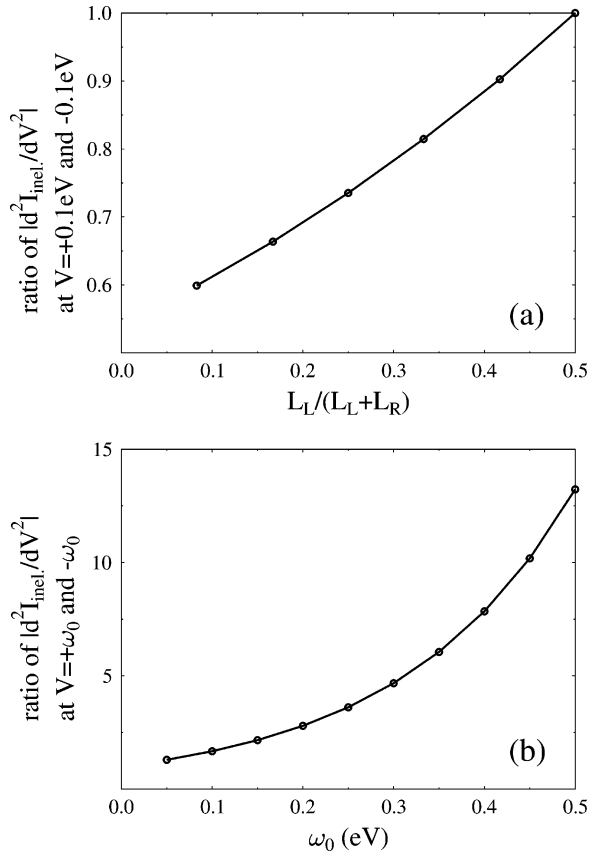


**Figure 3.** IETS asymmetry as a function of geometry and mode frequency. Zero-temperature lowest-order result from eq 7 calculation. (a) Ratio of $|d^2I/dV^2|$ at $V = +0.1$ V to $V = -0.1$ V as function of the vibrational mode position, $L_L/(L_L + L_R)$. Vibrational mode frequency is $\omega_0 = 0.1$ eV. (b) Ratio of $|d^2I/dV^2|$ at $V = +\omega_0$ to $V = -\omega_0$ as a function of the vibrational mode frequency, $\omega_0$. Vibrational mode is positioned at $L_L = 11$ Å, $L_R = 1$ Å.

different dependence on energy of $\Gamma_L$ and $\Gamma_R$ is seen to arise from different gap widths $L_L$ and $L_R$ that exist if the mode associated with the vibrational energy exchange is not positioned in the barrier geometric center. Other models for energy dependence of $\Gamma_K$, e.g., the Newns−Anderson model,[11] will similarly lead to asymmetric behavior for similar reasons.

In what follows, we demonstrate this behavior in simple model calculations for a junction characterized by a single molecular site between the electrodes. $d^2I/dV^2$ is obtained numerically from the function $I(V)$ calculated using the procedure described in Ref 8. The model parameters are $E_0 = 1$ eV, $E_F = 0$ eV, $\omega_0 = 0.1$ eV, $M = 0.3$ eV, and $\gamma_{ph} = 0.001$ eV. The parameters that determine self-energy (eq 10) are $A_K = 1$ eV and $U_K = 1$ eV ($K = L, R$), and $L_R = 1$ Å, $L_L$ is chosen to be 1 Å for the symmetric case and 11 Å for the asymmetric (STM-like) setup[3]. Figure 1 shows the zero-temperature lowest-order result for $d^2I/dV^2$ vs $V$ calculated from eq 7. It is seen that the STM-like geometry (Figure 1b) indeed gives an asymmetric IETS signal. It should be emphasized that asymmetry is predicted not only for STM-like setups, but also for junctions with overall symmetric structures when the relevant vibrational modes are not positioned symmetrically between the electrodes.

Figure 2 demonstrates the same effect when the Newns−Anderson model is used for the contact self-energies

$$\Gamma_K(E) = \begin{cases} \dfrac{V_K^2}{W_K}\sqrt{1-\left(\dfrac{E-E_K}{2W_K}\right)^2} & \left|\dfrac{E-E_K}{2W_K}\right| < 1 \\ 0 & \text{otherwise} \end{cases} \quad (11)$$

with $K = L, R$. We choose $V_L^2 = V_R^2 = 0.25$ eV$^2$, $W_L = W_R = 0.25$ eV, $E_R = 0$ eV, and $E_L = 0$ eV in the symmetric case (Figure 2a) and $E_L = 0.4$ eV in the asymmetric case (Figure 2b). Equation 8 is used in this calculation.

Finally, we investigate trends in the IETS asymmetry as a function of junction geometry and mode energy. Figure 3a shows the zero-temperature lowest-order result for ratio of $|d^2I/dV^2|$ at $V = +\omega_0$ to $V = -\omega_0$ ($\omega_0 = 0.1$ eV) as a function of the vibrational mode position in the junction. Equation 7 is used in calculations. Self-energy is taken in the form of eq 10 with the parameters of Figure 1. It is seen that stronger asymmetry in the position of the vibrational mode gives a more asymmetric IETS signal. Figure 3b shows the same ratio as a function of vibrational mode frequency for $L_R = 1$ Å and $L_L = 11$ Å. Higher-mode frequency leads to stronger asymmetry because of a more pronounced energy loss by the electron in the inelastic tunneling process.

We are not aware of systematic experimental efforts to study the phenomenon discussed above, but such experiments are obviously desirable. In a conclusive experiment, one should be able to associate observable IETS signals with vibrations that are known to be positioned asymmetrically in the junction and at the same time to verify that the regular I/V characteristic of the junction is itself symmetric. Also, it will be useful to be able to physically invert the molecular positioning in the junction (rather than to just reverse the potential bias) to distinguish the effects discussed in the work from possible extraneous small amplifier effects.

In conclusion, we have demonstrated within a simple model a possible mechanism for asymmetry in molecular IETS spectra

under voltage reversal. In contrast to the usual asymmetry of current−voltage characteristics, explained in terms of an asymmetric electrostatic potential profile across the junction at voltages of the order of the HOMO−LUMO gap, IETS experiments are done at much smaller biases. Within our nonequilibrium Green function approach, different energy dependences of the retarded self-energy associated with each molecule−contact coupling are identified as the possible cause of IETS asymmetry. The effect disappears when this energy dependence is the same, $\Gamma_L(E) = \lambda\Gamma_R(E)$. Finally, it should be pointed out that while we have used a simple model to demonstrate the origin of asymmetry in IETS signals, the NEGF theoretical framework described above can be used as a quantitative theoretical tool for realistic situations and can be extended to higher-order effects in electron−phonon interaction.

**Acknowledgment.** We are grateful to the DoD MURI/DURINT program, to the DARPA Moleapps program, to the United States-Israel Binational Science Foundation, the Wolkswagen Foundation, and the Israel Science Foundation for support of this work. This paper is dedicated to George Flynn, friend and mentor to much of the field of physical chemistry, outstanding scholar, and advocate for chemists and chemistry.

## References and Notes

(1) Kirtledy, J.; Scalapino, D. J.; Hansma, P. K. *Phys. Rev. B: Condens. Matter Mater. Phys.* **1976**, *14*, 3177−3184. Kirtley, J.; Hall, J. T. *Phys. Rev. B: Condens. Matter Mater. Phys.* **1980**, *22*, 848−856.

(2) Aviram, A.; Ratner, M. A. *Chem. Phys. Lett.* **1974**, *29*, 277−283. Martin, A. S.; Sambles, J. R. *Nanotechnology* **1996**, *7*, 401−405. Metzger, R. M. *J. Mater. Chem.* **2000**, *10*, 55−62. Stokbro, K.; Taylor, J.; Brandbyge, M. *J. Am. Chem. Soc.* **2003**, *125*, 3674−3675.

(3) Giancarlo, L.; Cyr, D.; Muyskens, K.; Flynn, G. W. *Langmuir* **1998**, *14*, 1465−1471. Claypool, C. L.; Faglioni, F.; Goddard, W. A., III; Gray, H. B.; Lewis, N. S.; Marcus, R. A. *J. Phys. Chem. B* **1997**, *101*, 5978−5995. Miura, A.; Chen, Z.; Uji-i, H.; De Feyter, S.; Zdanowska, M.; Jonkheijm, P.; Schenning, P. H. J.; Meijer, E. W.; Würthner, F.; De Schryver, F. C. *J. Am. Chem. Soc.* **2003**, *125*, 14968−14969.

(4) Mujica, V.; Ratner, M. A.; Nitzan, A. *Chem. Phys.* **2002**, *281*, 147−150. Galperin, M.; Nitzan, A.; Sek, S.; Majda, M. *J. Electroanal. Chem.* **2003**, *550−551*, 337−350.

(5) Zahid, F.; Ghosh, A. W.; Paulsson, M.; Polizzi, E.; Datta, S. *cond-mat/0403401*, 2004.

(6) Lambe, J.; Jaklevic, R. C. *Phys. Rev.* **1968**, *165*, 821−832. Hipps, K. W.; Mazur, U. *J. Phys. Chem.* **1993**, *97*, 7803−7814. Kushmerick, J. G.; Lazorcik, J.; Patterson, C. H.; Shashidhar, R.; Seferos, D. S.; Bazan, G. C. *Nano Lett.* **2004**, *4*, 639−642. Wang, W.; Lee, T.; Kletzschmar, I.; Reed, M. A. *Nano Lett.* **2004**, *4*, 643−646. Kushmerick, J. G.; Allara, D. L.; Mallouk, T. E.; Mayer, T. S. *MRS Bull.* **2004**, *29*, 396−402. Smith, R. H. M.; Noat, Y.; Untiedt, C.; Lang, N. D.; van Hemert, M. C.; van Ruitenbeek, J. M. *Nature* **2002**, *419*, 906−909.

(7) Bickers, N. E. *Rev. Mod. Phys.* **1987**, *59*, 845−939.

(8) Datta, S. *Electronic Transport in Mesoscopic Systems*; Cambridge University Press: Cambridge, 1997. Galperin, M.; Ratner, M. A.; Nitzan, A. *Nano Lett.* **2004**, *4*, 1605−1611. Galperin, M.; Ratner, M. A.; Nitzan, A. *J. Chem. Phys.* **2004**, *121*, 11965−11979.

(9) Note that the additive character of inelastic processes is correct only in the lowest order of perturbation theory and for the noncrossing approximation. In general, inelastic processes lead to renormalization of the elastic channel as well, so that name "inelastic" for this expression is not exact (see Caroli, C.; Combescot, R.; Nozieres, P.; Saint-James, D. *J. Phys. C: Solid State Phys.* 1972, *5*, 21−42 for detailed discussion). Note also, that elastic current renormalization due to the opening of an inelastic channel may lead to decrease (rather than increase) in the total current (see ref 8 and references therein).

(10) Datta, S.; Tian, W. D.; Hong, S. H.; Reifenberger, R.; Henderson, J. I.; Kubiak, C. P. *Phys. Rev. Lett.* **1997**, *79*, 2530−2533.

(11) Newns, D. M. *Phys. Rev.* **1969**, *178*, 1123−1135.